

Disrupting information coding via block of 4-AP-sensitive potassium channels

Krishnan Padmanabhan^{1,2} and Nathaniel N. Urban^{1,2,3}

¹Department of Biological Sciences, Carnegie Mellon University, Pittsburgh, Pennsylvania; ²Center for the Neural Basis of Cognition, Pittsburgh, Pennsylvania; and ³Department of Neuroscience, University of Pittsburgh, Pittsburgh, Pennsylvania

Submitted 18 November 2013; accepted in final form 30 May 2014

Padmanabhan K, Urban NN. Disrupting information coding via block of 4-AP-sensitive potassium channels. *J Neurophysiol* 112: 1054–1066, 2014. First published June 4, 2014; doi:10.1152/jn.00823.2013.—Recent interest has emerged on the role of intrinsic biophysical diversity in neuronal coding. An important question in neurophysiology is understanding which voltage-gated ion channels are responsible for this diversity and how variable expression or activity of one class of ion channels across neurons of a single type affects the way populations carry information. In mitral cells in the olfactory bulb of mice, we found that biophysical diversity was conferred in part by 4-aminopyridine (4-AP)-sensitive potassium channels and reduced following block of those channels. When populations of mitral cells were stimulated with identical inputs, the diversity exhibited in their output spike patterns reduced with the addition of 4-AP, decreasing the stimulus information carried by ensembles of 15 neurons from 437 ± 15 to 397 ± 19 bits/s. Decreases in information were due to reduction in the diversity of population spike patterns generated in response to different features of the stimulus, suggesting that the coding capacity of a population can be altered by changes in the function of single ion channel types.

biophysics; coding; diversity; K_v potassium channel; olfaction

NEURONS IN PRIMARY SENSORY areas encode stimuli with the patterns of their action potentials (spikes). Patterns of spiking are affected by a number of factors including the inputs to the cell (Rubin and Katz 1999; Meister and Bonhoeffer 2001; Dhawale et al. 2010), the location of those inputs on the dendrites (Häusser and Mel 2003; Jia et al. 2010), the morphology of the neuron (Mainen and Sejnowski 1996), and the voltage-gated channels expressed in each cell (Conner and Stevens 1971; Balu et al. 2004; Angelo and Margrie 2011). Neurons exhibit remarkable diversity in each of these features, and although all are important for neural computation, far less studied is the connection between intrinsic biophysical diversity and computation. Examples of experimental (Osborne et al. 2008) and theoretical work (Stocks 2000; Shamir and Sompolinsky 2006; Chelaru and Dragoi 2008) highlight the importance of response heterogeneity for neural coding, but often the focus is largely on heterogeneity at the circuit or synaptic level, rather than the variability of intrinsic properties.

In the main olfactory bulb (MOB), mitral cells are the principal relay neurons for conveying odor information from sensory receptors to areas such as the cortex and amygdala (Ghosh et al. 2011; Miyamichi et al. 2011; Sosulski et al. 2011). Recently, we have shown that diversity in mitral cell intrinsic properties allow populations to generate diverse spike patterns in response to a stimulus, thus improving the information ensembles carry about that stimulus (Padmanabhan and

Urban 2010; Tripathy et al. 2013). However, while the ion channels that are differentially expressed across mitral cells are being identified (Padmanabhan and Urban 2010; Angelo et al. 2012), the specific contribution of any one channel to the coding capacity of neuronal populations has not been evaluated.

To explore how diversity of voltage-gated ion channel across a population of neurons impacts coding, we recorded from mitral cells from different glomeruli in the MOB of mice, where an inactivating potassium current sensitive to low concentrations of 4-aminopyridine (4-AP) has been reported to influence neuronal firing (Balu et al. 2004) and where diversity has been shown to be important for neural coding (Padmanabhan and Urban 2010). As the axons of mitral cells from different glomeruli converge onto individual piriform cortical neurons (Miyamichi et al. 2011), we focused on how cell-to-cell diversity affects neuronal coding from the perspective of interglomerular diversity. In this framework, diversity across mitral cells from different glomeruli would be integrated by individual piriform cortical neurons to encode for odor information. We found that the heterogeneity of mitral cell responses from different glomeruli was reduced by blockade of potassium channels with 5 μ M 4-AP. By effectively equalizing 4-AP-sensitive current densities to zero, the information carried by ensembles of mitral cells was decreased by up to 21%. By reducing the diversity of a single channel, thereby reducing this biophysical feature's heterogeneity across the population, our results highlight the role that ion-channel diversity plays in information encoding. Further, this work suggests that variability of an individual channel's activity (at the physiological level as we have measured in the work, but also possibly at the molecular and cellular level) across the population may be one mechanism by which neuronal circuits control their coding capacity.

MATERIALS AND METHODS

Animal procedures. All procedures were done as previously described and in accordance with the guidelines for the care and use of animals at Carnegie Mellon University, which approved the study. Briefly, C57Bl/6 mice of either sex between postnatal day (P)12 and P18 were deeply anesthetized with isoflurane and then decapitated. Brains were placed in ice-cold Ringer's solution (concentrations in mM = 125 NaCl, 25 glucose, 2.5 KCl, 25 NaHCO₃, 1.25 NaH₂PO₄, 1 MgCl₂, and 2.5 CaCl₂). Three-hundred-micrometer coronal sections of the bulb (VT1000S; Leica, Nussloch, Germany) were made and incubated in Ringer's at 37°C for 30 min before recording.

Electrophysiology. Whole cell patch recordings filled with an internal buffer concentration (130 mM potassium gluconate, 10 mM HEPES, 2 mM MgCl₂, 2 mM Mg-ATP, 2 mM Na₂ATP, 0.3 mM GTP, 4 mM NaCl, and in some cases 10–50 μ M Alexa 488/594 Hydrazide or 1% biocytin) were made using a Multiclamp 700A amplifier (Molecular Devices, Palo Alto, CA) and an ITC-18 acqui-

Address for reprint requests and other correspondence: N. N. Urban, Dept. of Biological Sciences, Carnegie Mellon Univ., Pittsburgh, PA 15213 (e-mail: nurban@cmu.edu).

sition board (Instrutech, Port Washington, NY). Mitral cells were identified under IR-DIC optics based on laminar position in the MOB and confirmed with fluorescent intracellular fills. One neuron was recorded per slice, and between one and three neurons were recorded from each animal. Neurons from different slices belonged to different glomeruli. All experiments were done at 35°C in Ringer's solution with excitatory (25 μ M APV and 10 μ M CNQX) and inhibitory (10 μ M bicuculline) synaptic activity blocked.

A hyperpolarizing pulse was injected before stimuli to measure input resistance (IR) and assess recording stability. In all experiments, series resistance was compensated for. As recordings near in vivo temperatures can degrade the slice, the hyperpolarizing pulse was delivered before each trial across the entire recording period to ensure that the cells remained stable and recordings did not degrade over the duration of the experiment. Recording stability was also assessed by comparing the spike patterns recorded at the beginning of experiment (first trial) with those at the end of the experiment (last trial) to the same stimulus. Furthermore, we measured the stability of the recordings throughout our experiments, monitoring the resting membrane potential that varied 2.6 ± 1.7 mV from the beginning of the trial to the end of the trial in the control condition and varied 1.8 ± 1.3 mV over the duration of the 4-AP recordings. Additionally, we tracked both the IR and the membrane time constant over the duration of the recordings. Neurons had an IR of 108 ± 44 M Ω in the control condition and an IR of 90 ± 36 M Ω following the addition of 4-AP, with the change in IR being significant in 72% of the neurons ($n = 13/18$; $P < 0.05$, ANOVA). The IRs recorded across the population of mitral cells were consistent with values previously reported (Cang and Isaacson 2003; Abraham et al. 2010).

Stimulus. To generate frozen noise stimuli, white noise with a mean amplitude of 150–200 pA and a standard deviation of 40 pA was generated for 2.5 s. This stimulus was then convolved with an alpha function of the form $t \times (\exp(-t/\tau))$, where $\tau = 3$ ms. The resultant stimulus has previously been shown to be optimal for generating reliable spike trains across various trials (Bryant and Segundo 1976; Mainen and Sejnowski 1997; Gálan et al. 2008). This stimulus was presented to neurons for 2.5 s over multiple trials, with an intertrial interval of 8 s.

Principal component analysis. The fluctuating noise stimulus described above was delivered to neurons in both the control and the 4-AP condition over multiple trials (control = 42.7 ± 18.8 trials; 4-AP = 33.1 ± 15.9 trials) for 2.5 s. The resultant spike trains from all neurons ($n = 23$ neurons from 23 slices from 10 animals) in all conditions (control and 4-AP) were transformed into binary vectors of 1s (corresponding to the occurrence of a spike) and 0s (absence of a spike) in 1-ms bins. As all recorded neurons received the same stimulus for both the control and the 4-AP condition, we aligned all the spike train vectors to generate a matrix M of size spike trains (s) \times time (T) in size. On this data, we calculated the covariance matrix (C), (T) \times (T) in size. We then performed eigenvalue decomposition on the covariance matrix C to acquire the eigenvalues and eigenvectors of the original data. We projected each spike train [a vector of length (T)] onto the first and second principal component (PC) by taking the dot product of the spike train and the eigenvector. From this, each spike train was represented as a point, and the spike trains from different neurons were represented with the same color. Because the eigenvectors for both the control and the 4-AP conditions were determined from a covariance matrix containing each spike train from all the trials from all cells in both conditions, the basis vectors corresponding to the first two PCs are the same for the two conditions. All analysis was performed using MATLAB.

K-nearest neighbor analysis. To determine the degree to which spike trains across trials from a single cell and across different cells was more or less similar, we employed a K -nearest neighbor (KNN) analysis. Spike trains from the control and 4-AP condition were projected onto the first 30 PCs (PC1–30) as calculated above. From this, individual trials were separated into test and train conditions (the

number of trials in the training ranging from 30 to 70% of the total spike trains for the control and the 4-AP condition). A random test trial was selected and either the 5 nearest neighbors of the 15 nearest neighbors (calculated by measuring the Euclidian distance between the test trial and all the training trials) were used to determine the trial's identity. If the test trial's identity determined by the nearest neighbors was the same as the test trial's true identity, then this was termed as a successful classification. The percent correct was measured as a fraction of the correct test trials in the two conditions. The KNN classification was performed on 100 repeats of the data for each condition (number of trials in testing vs. training, dimensions, and number of nearest neighbors) to estimate the performance of the classification algorithm.

Information calculation. Stimulus information, or mutual information, was calculated as the difference between the total entropy and the noise entropy as described previously (Osborne et al. 2008; Padmanabhan and Urban 2010).

First, spike trains from individual trials in each cell were binned and binarized in 8-ms nonoverlapping windows and aligned to the stimulus. Spike trains from each neuron were thus represented as a binary spike train vector of 1 and 0 s. Spike train vectors from different mitral cells were assembled into a model population response (as has been done previously, see Padmanabhan and Urban 2010) by randomly selecting spike train vectors for each population in the cell and turning this into a spike train matrix A whose dimensions are neurons (n) by time (T). This was repeated over multiple resamplings of the data to estimate the ensemble of neurons information content about the stimulus at any given time (noise entropy, H_{noise}) and over all of the stimuli (total entropy, H_{total}).

$$I = H_{\text{total}} - H_{\text{noise}} \quad (1)$$

To do this, we examined the binary words, or patterns of 1 and 0 s across the each different ensemble of neurons at each time point. For instance, in a three-cell population, if neurons 1 and 3 fired at time $t = 1$ for one trial, then that word would for that trial would be $a_1[1 \ 0 \ 1]$. We generated for different model populations a probability distribution of the words that occur at each time, and estimate the noise entropy as the mean of noise entropy at each time t

$$H_{\text{noise}} = -\frac{1}{T} \sum_{t=1}^T \sum_{n=1}^N P(a_n | S_t) \log_2 P(a_n | S_t) \quad (2)$$

where a_n = pattern n at stimulus time S_t . The noise entropy is then subtracted from the stimulus entropy

$$H_{\text{total}} = -\sum_{n=1}^N P(a_n) \log_2 P(a_n) \quad (3)$$

For comparison of firing rate matched ensembles, only populations where the mean spike rate of the neurons in the six-cell ensemble was ~ 20 Hz were included.

RESULTS

Whole cell patch-clamp recordings were made in mitral cells from slices of mouse olfactory bulb (P12–18). To separate the role of intrinsic diversity in affecting spiking activity from the role of synaptic input, including recurrent inhibition (Urban and Sakmann 2002), all recordings were made in the presence of synaptic blockers (see MATERIALS AND METHODS). Mitral cells were held at -59 ± 2 mV ($n = 12$ cells; $n = 7$ animals) throughout the recordings, which is similar to the resting membrane potentials that have been reported in vivo (Cang and Isaacson 2003). Consistent with previous results, direct current injections to mitral cells ($I = 150$ – 250 pA; $n = 3$ trials/cell, 2-s duration) resulted in some neurons firing regularly [coefficient of variation of the interspike interval (CV_{isi}) < 0.2 ; Fig. 1B, *top*] and others firing in bursts ($CV_{\text{isi}} > 0.4$; Fig. 1B, *bottom*)

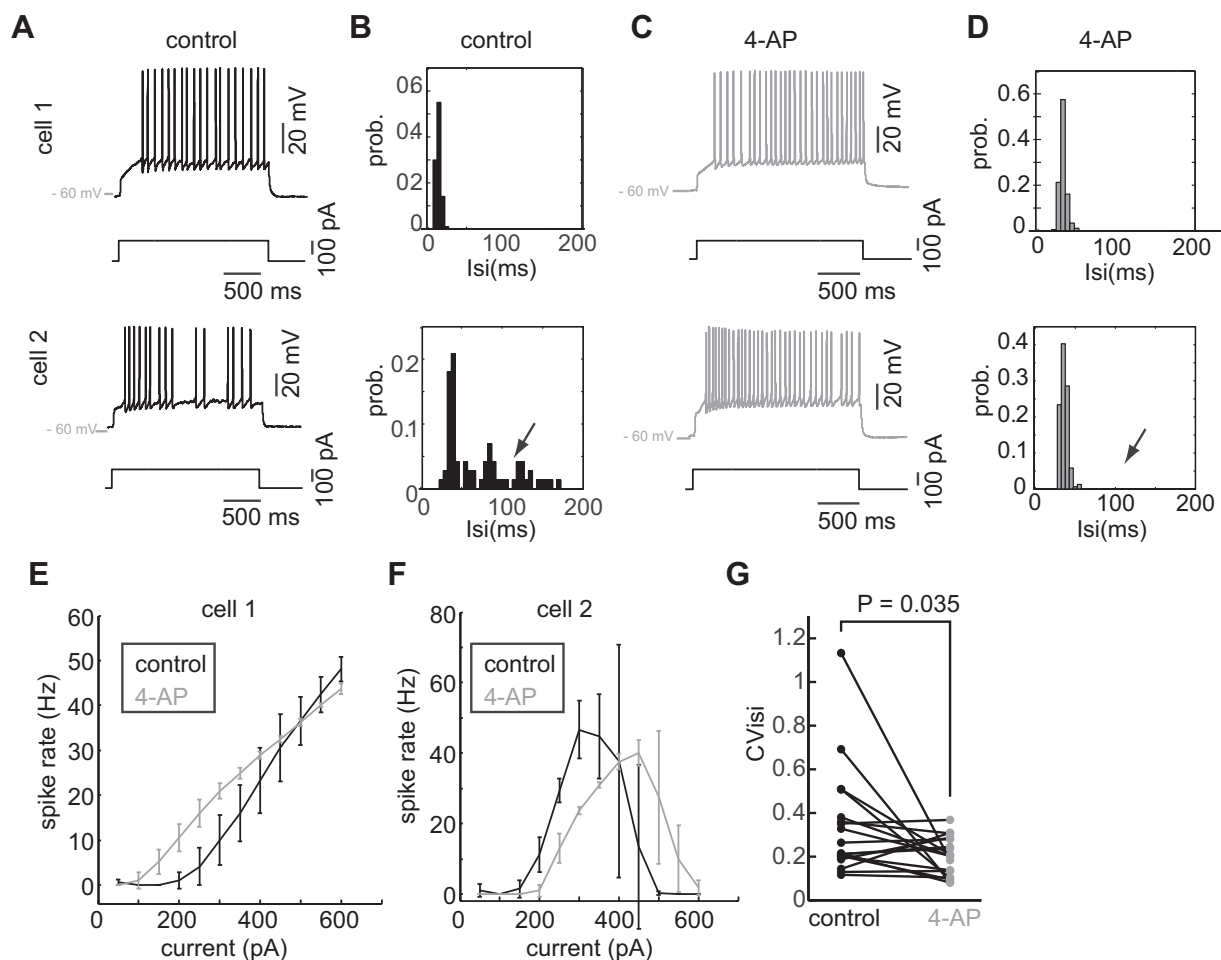


Fig. 1. Mitral cell diversity is conferred in part by a 4-aminopyridine (4-AP)-sensitive potassium channel. *A* and *C*: spike responses to DC current from 2 recorded mitral cells in the control condition (*A*) and with the addition of 4-AP (*C*). *B* and *D*: interspike interval histograms for the cells in control condition (*B*) and with the addition of 4-AP (*D*). *E*: population coefficient of variation in the interspike intervals (CV_{isi}) show a decrease in the distribution of CV_{isi} with the addition of 4-AP. *F* and *G*: firing rate/current (F/I) relationship for the 2 cells in *A*.

(Padmanabhan and Urban 2010). Previous work has shown that burst-like firing in mitral cells can be altered by blockade of a 4-AP-sensitive potassium channel (Balu et al. 2004). We wished to confirm these previous results and determine if this potassium channel accounted for some of the differences observed in neuronal responses. Following perfusion of 5 μ M 4-AP for 10 min, mitral cells were held at -58 ± 4 mV ($n = 12$), which was not significantly different from the voltage cells were held at in the control condition ($P = 0.41$, ANOVA). Extracellular bath application of 5 μ M 4-AP (Balu et al. 2004) had little effect on some cells, which continued to fire regularly (Fig. 1*C*), leaving their CV_{isi} s unchanged (Fig. 1*D*, top; $CV_{isi} = 0.11$). However, other neurons were affected by 4-AP, no longer exhibiting “bursty” firing patterns (Fig. 1*C*, bottom), and consequently, these cells had a much lower CV_{isi} s (Fig. 1*D*; $CV_{isi} = 0.23$). In the population of recorded mitral cells ($n = 12$), we found a significant change in the CV_{isi} s following the addition of 4-AP (Fig. 1*E*; Control $CV_{isi} = 0.34 \pm 0.25$; 4-AP $CV_{isi} = 0.20 \pm 0.09$; $P = 0.035$, Wilcoxon rank sum test), suggesting that differential expression of a 4-AP-sensitive potassium channel across the population was one source of diversity.

4-AP also affected each mitral cell’s firing rate to different current injections. In the example *cell 1*, the firing rates

at lower current injections (<400 pA) were increased slightly with the addition of 4-AP (Fig. 1*F*). By contrast, *cell 2* saw a decrease in the firing rate particularly at lower current injection amplitudes (Fig. 1*G*) but saturated at higher current injections in both the control (black traces) and 4-AP conditions (gray traces, Fig. 1*G*; >400 pA). Taken together, the effect of 4-AP on the current of the neuron to firing rate relationship (F/I curve) was highly varied, illustrating the complex effect that 4-AP-sensitive potassium channel had on shaping the neural response, particularly across a population of cells that was diverse for this intrinsic property.

Blocking a source of biophysical diversity alters coding. Although DC current input identified one channel that accounted for some of the diversity we saw, the effects on spike responses (bursting for instance) and the effects on firing rate made studying neural coding difficult using this relatively simple stimulus. Additionally, previous work has shown that a DC current is ill suited for studying how a neuron or population of neurons encodes a dynamic stimulus (de Ruyter van Steveninck et al. 1997) including how spike trains may convey information about a stimulus (Strong et al. 1998). Thus, to examine the role of channel diversity in coding, we injected a frozen noise current (white noise convolved with a 3-ms alpha

function; DC bias = 150–250 pA; sigma = 40 pA; tau = 3 ms; Fig. 2, *A* and *B*), which has been shown to be optimal for generating spike times that are reliable from trial-to-trial in mitral cells (Galán et al. 2008). The stimulus generated a complex pattern of firing in both control conditions (Fig. 2*A*,

bottom) and following the addition of 4-AP (Fig. 2*B*, *bottom*). Repeated presentation of this stimulus resulted in reproducible spike patterns in both the control condition (Fig. 2, *C–E*, black) and with the addition of 4-AP (Fig. 2, *C–E*, gray). However, comparing spike trains from individual neurons in the two

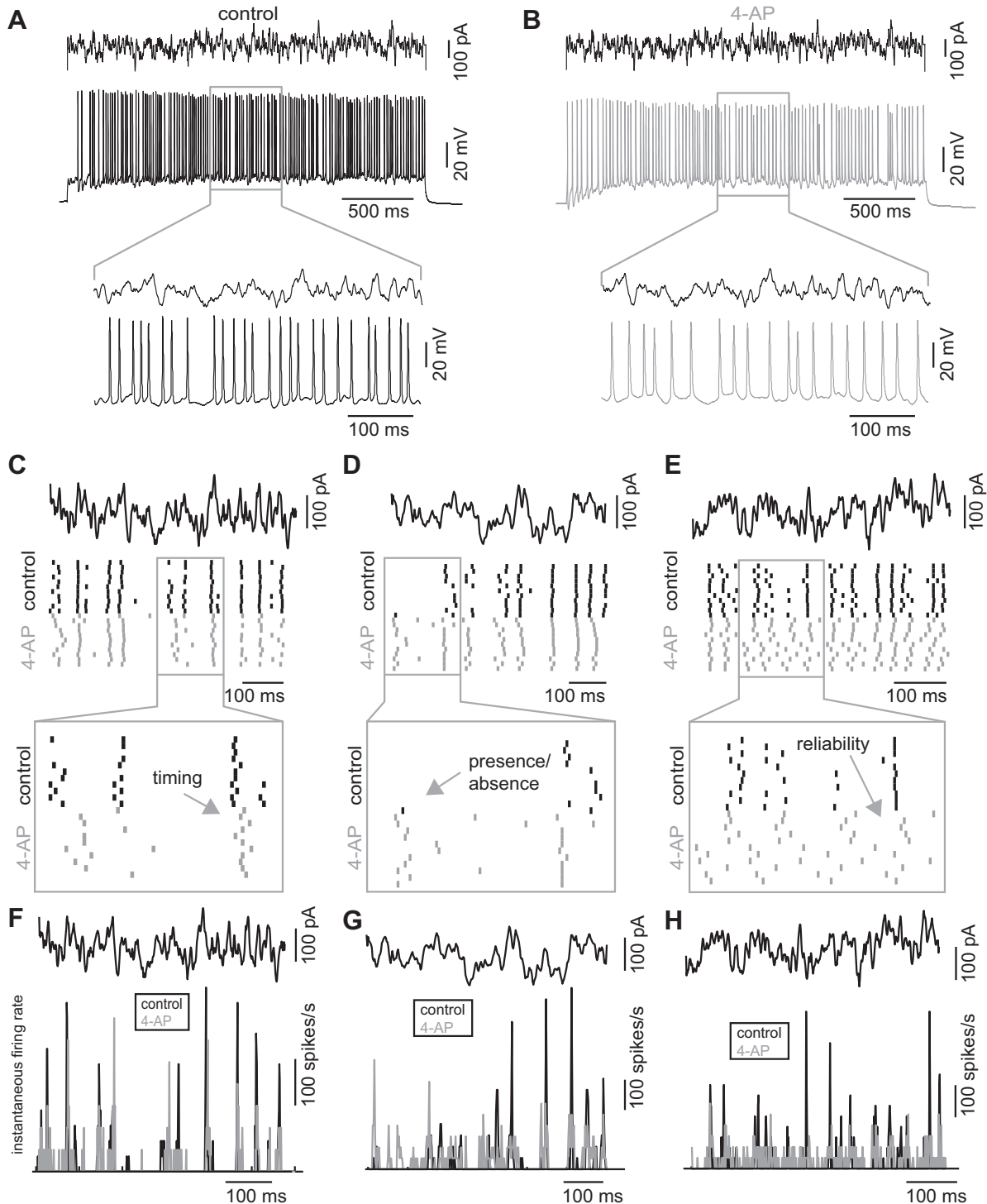


Fig. 2. Frozen noise current input causes variable firing patterns in mitral cells. *A* and *B*: representative trace of a cell's response (*bottom*) to a frozen noise stimulus (*top*) in the control (*A*) condition and following the addition of 4-AP (*B*). *C–E*: frozen noise current delivered to 3 mitral cells (*top* black trace). Spike responses of the mitral cells to the current in *A–C* in the control condition (black) and with the addition of 4-AP (gray) over 11 repeated presentations of the stimulus. Enlargement (gray boxes, *bottom*) highlight the differences in neuronal responses in the 2 conditions including differences in timing (*C*), the presence or absence of a spike (*D*), and the reliability of spiking (*E*). *F–H*: instantaneous firing rate is modulated over a broad range by the input current for both the control and 4-AP conditions.

conditions revealed how responses were altered following 4-AP block. For instance, 4-AP altered the timing of spike responses to the stimulus (Fig. 2C, *bottom box*, arrow), whether or not a cell responded to a specific portion of the stimulus (Fig. 2D, *bottom box*, arrow) or the reliability with which spikes occurred to the stimulus (Fig. 2E, *bottom box*, arrow). Collectively, blocking 4-AP-sensitive potassium channels altered the responses patterns of each neuron, thereby changing how the stimulus was encoded for in the patterns of spiking. As recordings were made in the presence of synaptic blockers, the changes observed in the spike responses to 4-AP were not due to differences in the synaptic input across conditions. Finally, peristimulus time histograms of the spike responses to the stimulus showed that instantaneous firing rates were modulated over a broad range (de Ruyter van Steveninck et al. 1997) in both the control condition (Fig. 2, *F–H*, black traces) and with the addition of 5 μ M 4-AP (Fig. 2, *F–H*, gray traces). Importantly, this variability of the instantaneous firing rate was preserved in the presence of 4-AP, confirming that blocking

4-AP-sensitive potassium currents did not compromise coding trivially, by say simply preventing the neuron from spiking.

Changes in the patterns of spiking reflected by alterations in instantaneous firing rates suggested that blocking 4-AP-sensitive channels altered how individual neurons represented the stimulus. However, in the context of olfactory coding, populations of mitral cells synapse onto piriform cortical neurons, a pattern of connectivity that motivated how we explored the effect of information transmission by populations of mitral cells. To do this, an identical frozen noise current (duration 2.5 s) was injected into each neuron ($n = 23$ mitral cells; $n = 10$ animals) over multiple trials (control = 42.7 ± 18.8 trials; 4-AP = 33.1 ± 15.9 trials) in control conditions and following blockade of potassium channels by 4-AP. The spike trains for the 23 cells (where each color corresponded to an individual neuron) were then represented as spike rasters (Fig. 3A) in both the control (Fig. 3A, black) and 4-AP (Fig. 3A, red) conditions for a 2-s window of the stimulus (Fig. 3A, black current trace). Given the complex patterns of spiking found both across

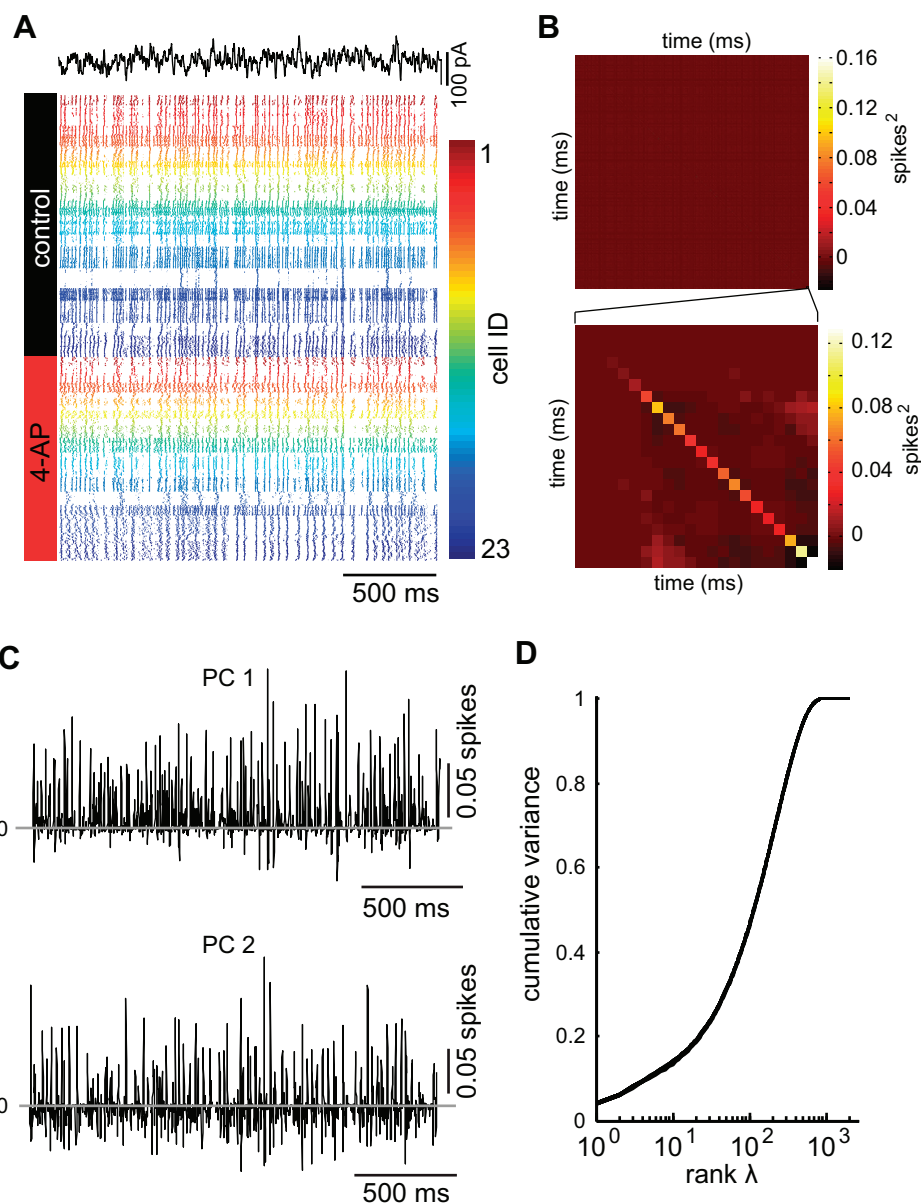


Fig. 3. Representing spike trains in a low dimensional space. *A*: spike responses to a rapidly fluctuating current (black trace) for 23 neurons (color coded) in both the control condition (black) and the 4-AP condition (red). *B*: covariance matrix for the spike trains in *A* (*top*) and an enlargement of the last 22 ms of the covariance matrix (*box*). *C*: first 2 principal components (PC1, *top*; PC2, *bottom*) calculated from all the spike trains from all the recorded neurons in all the conditions (control and 4-AP). *D*: cumulative variance explained by each of the eigenvalues (ranked).

neurons and across conditions, we wanted to develop an alternative way to visualize the similarities and differences of the spike patterns within trials of a single neuron and across the different neurons. To do this, we transformed spike trains into binary vectors of 1 and 0 s and then calculated the covariance matrix (Fig. 3B) for all the trials from all the cells in both conditions (control and 4-AP). From this, we determined the first two PCs (PCs) of the spike train data (Fig. 3C) corresponding to the first two eigenvectors of the covariance matrix by performing eigenvalue decomposition. In addition, we plotted the cumulative variance explained by ranking the eigenvalues (Fig. 3D). PC1 and PC2 illustrated the complexity of responses across the population (Fig. 3C) and also revealed that neuron-to-neuron differences were not due simply to differences in the firing rates over time (neurons adapting to the stimulus). Furthermore, as the majority of the variance of the firing patterns could be explained in far fewer dimensions (<100) that the original data (2,000 dimensions), projecting

spike trains in the space defined by the PCs allowed us to visualize the spike train response heterogeneity across the population of neurons in lower dimensional space while still capturing the underlying differences of those responses.

Each spike train vector was projected onto a space defined by the first two PCs and although this low-dimensional representation did not account for the full variance of the responses, it did reveal both the response diversity across trials in a single mitral cell (Fig. 4, A and B, points) as well as the diversity to responses across trials from different neurons (Fig. 4, A and B, colors).

In this space, mitral cell spike patterns recorded in the control condition were more widely distributed in both PC1 [SD = 32.4 ± 0.2 arbitrary units (AU)] and PC2 (SD = 21.3 ± 0.3 AU) than following the addition of 4-AP (PC1: SD = 11.4 ± 0.3 AU; PC2: SD = 8.6 ± 0.1 AU; $P < 0.005$ PC1 and $P < 0.005$ PC2, ANOVA; $n = 981$ control; $n = 761$ 4-AP; 50 resamples, bootstrap with replacement). Consistent with the

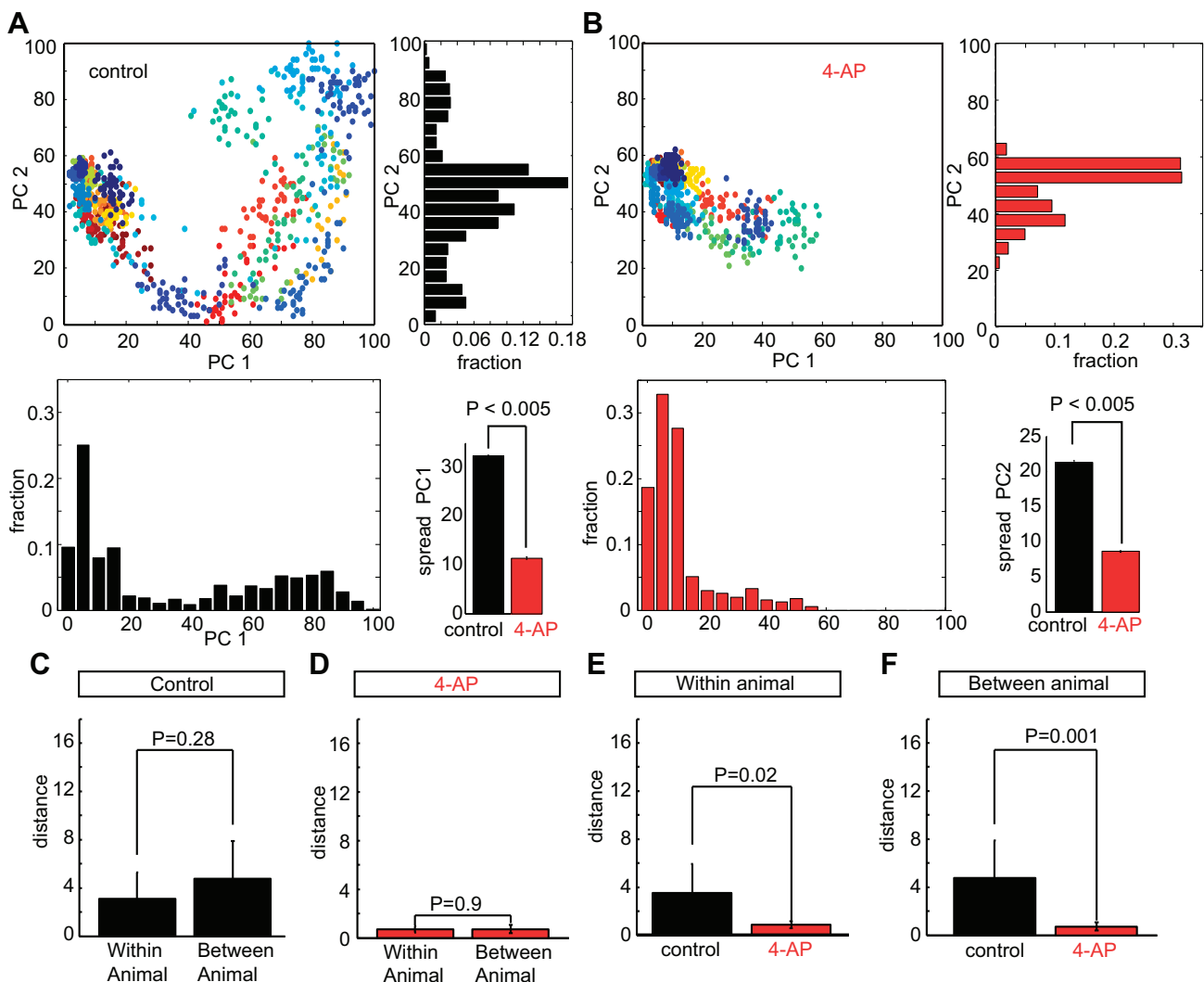


Fig. 4. 4-AP decreases spike pattern diversity in mitral cells. A and B: spike responses in the control condition (A, top left) and in the presence of 4-AP (B, top left) to a 2-s frozen noise stimulus projected onto the space defined by the first 2 PCs. Each point is a trial, each color corresponds to a single mitral cell. A and B: distribution of responses in the 2 conditions along PC1 (bottom left) and PC2 (top left) with the decrease in the SD along both PC1 (A, bottom right) and PC2 (B, bottom right) illustrating the decrease in spike pattern diversity. Mean distance of spike trains from pairs of neurons within a single animal and between 2 different animals in the control condition (C) and following the addition of 4-AP (D). 4-AP reduces the diversity of spike train responses in a single animal (E) and across pairs of neurons from different animals (F).

reduction in diversity in response to DC inputs (Fig. 1), the spike responses to the same frozen noise stimulus in the 4-AP condition were less variable than those in the control condition. The mean pair-wise Euclidian distance between the projections of all spike patterns from a given cell to the spike patterns of every other cell was significantly larger ($P < 0.005$, ANOVA) in the control condition (distance = 47.8 ± 28.9 AU) compared with the 4-AP condition (distance = 15.8 ± 13.2 AU). Secondly, the response variability across trials within a single cell was significantly reduced ($P < 0.005$, ANOVA) following 4-AP block (average distance = 4.3 ± 4.4 AU) compared with controls (10.0 ± 11.0 AU). Taken together, 4-AP had multiple effects on the spike responses across populations of neurons. On the one hand, spike patterns between cells were more similar, resulting in fewer distinct representations of the stimulus. On the other hand, spike patterns within cells were more similar trial-by-trial, resulting in more reliable representations of the stimulus.

As the diversity described came from different animals ($n = 10$ animals), we wished to ensure that heterogeneity was a real property of within animal variability rather than between animal variability. To do this, we examined the spike trains of animals where we had recorded three neurons in each mouse ($n = 6$ neurons total) and compared the response variability from cells within the same animal to the response variability from the same cells across the animals ($n = 9$ pair-wise comparisons, $n = 6$ neurons). This was done by measuring the mean pair-wise distance of spike train projections onto PCs from neurons within the same animal ($n = 6$ pairs) and between different animals ($n = 9$ pairs). With greater mean distance, neuronal responses are more diverse. First, when we compared the response diversity of pairs of neurons ($n = 6$ pairs) within the same animal to that of pairs of neurons from different animals ($n = 9$ pairs), we found no significant difference in either the control (Fig. 4C; $P = 0.28$, ANOVA) or the 4-AP condition (Fig. 4D; $P = 0.9$, ANOVA), suggesting that the diversity we observed in mitral cell responses was not an artifact of sampling from different mice. When we then compared the responses of mitral cells from the same animal before and following the addition of 4-AP (Fig. 4E, $n = 6$ pair-wise comparisons), we found a significant decrease in the mean distance of spike train responses within the same animal ($P = 0.02$), suggesting that 4-AP was reducing response heterogeneity within individual animals. Similarly, when we calculated the mean spike train distances in the same six neurons across the different animals (Fig. 4F; $n = 9$ pair-wise comparisons), we found a significant decrease in the mean spike train distances ($P = 0.01$). This decrease in heterogeneity is consistent with our findings across all the mitral cells recorded ($n = 23$ neurons from 10 animals). Together, our results suggest that 4-AP block decreases diversity among mitral cells recorded in a single animal (Fig. 4E) similar to the decrease in the diversity across all cells from all animals (Fig. 4, B and F). This is also consistent with previous work that demonstrated diversity within the bulb of individual animals (Angelo et al. 2012) and suggests that the effects of 4-AP reflect decreases in the response variability within populations of mitral cells in the olfactory bulb of individual mice.

To further quantify the differences in patterns of spike trains between neurons in the control and the 4-AP condition, we performed a KNN classification on the spike trains projected

into the space of PCs. Classification was performed on the spike trains in Fig. 4. We ensured that both control and 4-AP spike trains were being compared in the space defined by the same PCs (calculated from all the spike trains from all the neurons in both the control and 4-AP condition) so as not to introduce any artifacts to the classification. Many parameters affect the classification accuracy of the KNN algorithm, including the dimensionality of the data, the number of nearest neighbors used to perform the classification, and the number of examples in the training and test sets. First, we found that the dimensionality of the data had a significant impact on classification performance for both the control and 4-AP conditions. Whereas KNN performed on the spike trains in the first two PCs (as visualized in Fig. 4) was 0.52 ± 0.02 in the control condition and 0.40 ± 0.02 in the 4-AP condition, the classification accuracy improved to 0.75 ± 0.02 in the control condition and 0.55 ± 0.02 in the 4-AP condition as the number of dimensions was increased to 30 when either 5 neighbors (Fig. 5A) or 15 neighbors (Fig. 5C) were used to classify the testing. However, in all conditions, we found that classification accuracy in the control population was always significantly higher than classification accuracy in the 4-AP population ($P < 0.05$, 2 dimensions; $P < 0.05$, 30 dimensions, ANOVA). We next wished to determine if the differences in the classification performance of the KNN algorithm in the control vs. the 4-AP conditions were simply due to differences in the number of the spike trains that seeded the training set. Across training sets that constituted 30, 50, and 70%, respectively, of the total data, the KNN was significantly better at classifying the spike train projections in the control condition compared with the 4-AP condition (Fig. 5B) when either the 5 nearest neighbors or the 15 nearest neighbors were used ($P < 0.0005$, ANOVA). Together, these data provided us with a quantitative description of the spike train differences in the control vs. the 4-AP condition; spike patterns between cells were made more similar following the addition of 4-AP, effectively making it more difficult for the KNN classification algorithm to correctly assign test spike trains to the correct cell.

As 4-AP block of potassium channels can affect both the active and passive properties of the neuron (Balu et al. 2004), we wished to determine if the changes in the spiking activity observed could be attributed simply to changes in the passive properties of neurons, such as their IR. To do this, we first visualized the spike trains from different trials in both the control (Fig. 6A, top, and B, top) and 4-AP (Fig. 6A, bottom, and B, bottom) condition. Two trials from each condition (trial 9 and trial 21), separated by 7 min in recording time, were used to visualize how spike responses to a frozen noise stimulus changed both within trials and between trials for neurons with different passive properties, including cells where the IR changed significantly following the addition of 4-AP (Fig. 6C; $P < 0.05$ ANOVA) and those where such changes were not observed (Fig. 6D). In the example cell (Fig. 6, A and C), where a significant change in the IR was observed, the spike train responses also changed following the addition of 4-AP. By contrast, in cell 2 (Fig. 6, B and D), neither the IR nor the spike trains appeared to change following the addition of 4-AP. To further explore the connections between the spike responses and neuronal passive properties, we examined how much changes in the pattern of spiking following 4-AP addition could be attributed to changes in the IR. To do this, we plotted

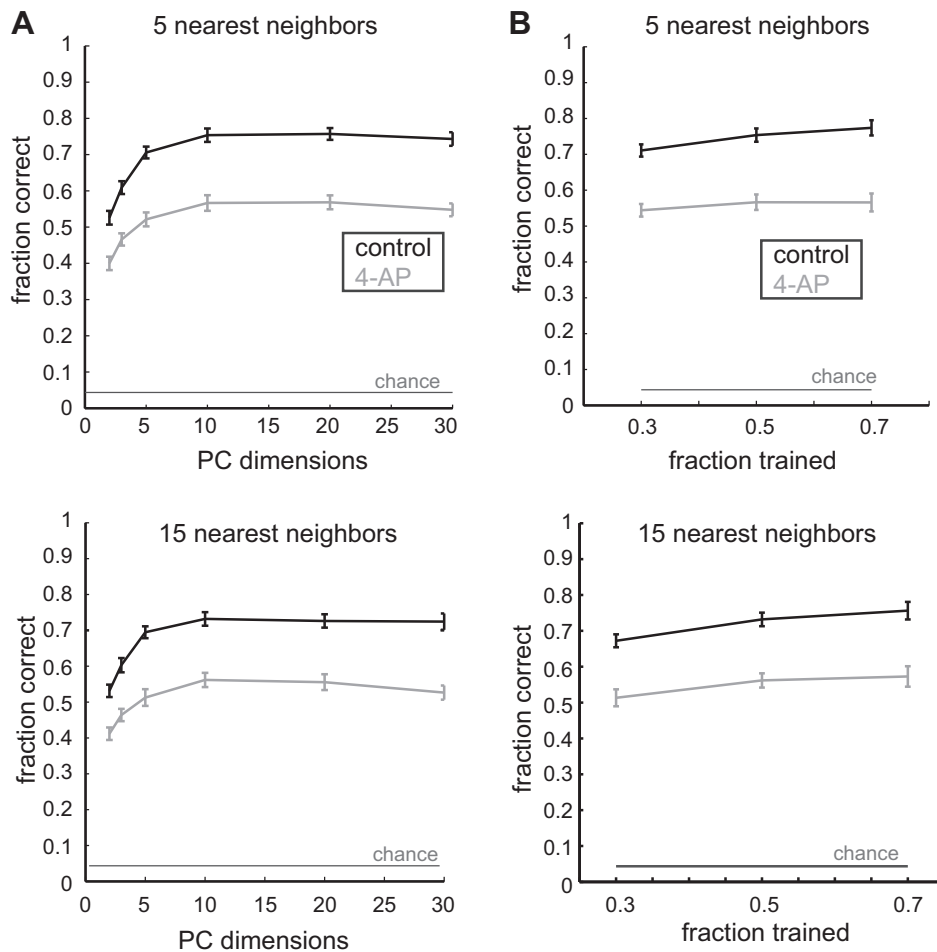


Fig. 5. *K*-nearest neighbor classification of spike trains. *A*: classification accuracy as a function of PC dimensions used for 5 nearest neighbors (*top*) and 15 nearest neighbors (*bottom*). *B*: effect of fraction of trials used for training when 5 nearest neighbors (*top*) and 15 nearest neighbors (*bottom*). Control is in black, 4-AP is in gray, and chance percentage is shown.

the relationship (Fig. 6*E*) between the change in the IR [IR_D ($M\Omega$), calculated as the Euclidian distances of the IR between the control and the 4-AP condition] for the neuron and the change in the patterns of spiking [PC_D (AU) calculated as the Euclidian distance between the PC projections of the spike trains before and after the addition of 4-AP for each cell]. We found no significant correlation ($P = 0.38$; $n = 18$) between the alterations in the IR of the neurons and the alterations in their spiking patterns (Fig. 6*E*), suggesting that changes in IR alone could not account for the changes in the spiking responses of these neurons following 4-AP addition.

The blocking of 4-AP-sensitive channels across populations of mitral cells had the effect of changing neurons responses in complex ways. All of these changes in spike responses, the variability across different cells, the similarity within cells over different trials, the firing rate of the neurons, and the collectively affect a population's ability to encode a stimulus. Although these spike train differences visualized across the whole stimulus (Fig. 3) over long time intervals (2 s) correspond to the timescales of long-latency inhibition (Urban and Sakmann 2002), they may not adequately reflect coding on other time scales, like the 10 s of milliseconds corresponding to the timing of single spikes (Smear et al. 2011), or the 100-ms time scales corresponding to the sniffing behaviors in mice (Carey and Wachowiak 2011). To capture coding independent of the specific stimulus used, and to understand coding on different time scales, including representing all of the observed changes

in spike patterns following the addition of 4-AP into a single value, we turned to an information theoretic metric (Osborne et al. 2008).

Conceptually, we wished to understand how the ensemble activity of mitral cells (from different glomeruli) related information about the stimulus to postsynaptic targets in the piriform cortex. The information in mitral cell population responses was calculated for populations of neurons ranging from 2 to 15, randomly drawn from the recorded set of mitral cells ($n = 23$) as described previously (Padmanabhan and Urban 2010). To perform this calculation, we presented an identical stimulus to each of the cells in our population in both the control and 4-AP condition over multiple trials (Fig. 7*A*). Stimuli were presented for 2.5 s each (but for analysis of the spike train information content, we only included the middle 2 s of the responses to discard transient stimulus onset artifacts). An example response trial from three example cells (Fig. 7*A*, *top*, black, green, and blue) to the stimulus (Fig. 7*A*, black trace) and spike rasters for the same three cells over multiple stimulus presentations illustrate both the variability of responses across a single cell and the variability of responses across different neurons (Fig. 7*A*, spike rasters). We then recorded the responses of the same three example neurons to the same stimulus following the addition of 4-AP (Fig. 7*A*, *bottom*, black, green, and blue) over multiple trials (Fig. 7*A*, *bottom*, spike rasters). To determine the entropy (both the noise and the total), individual trials for each neuron were drawn at

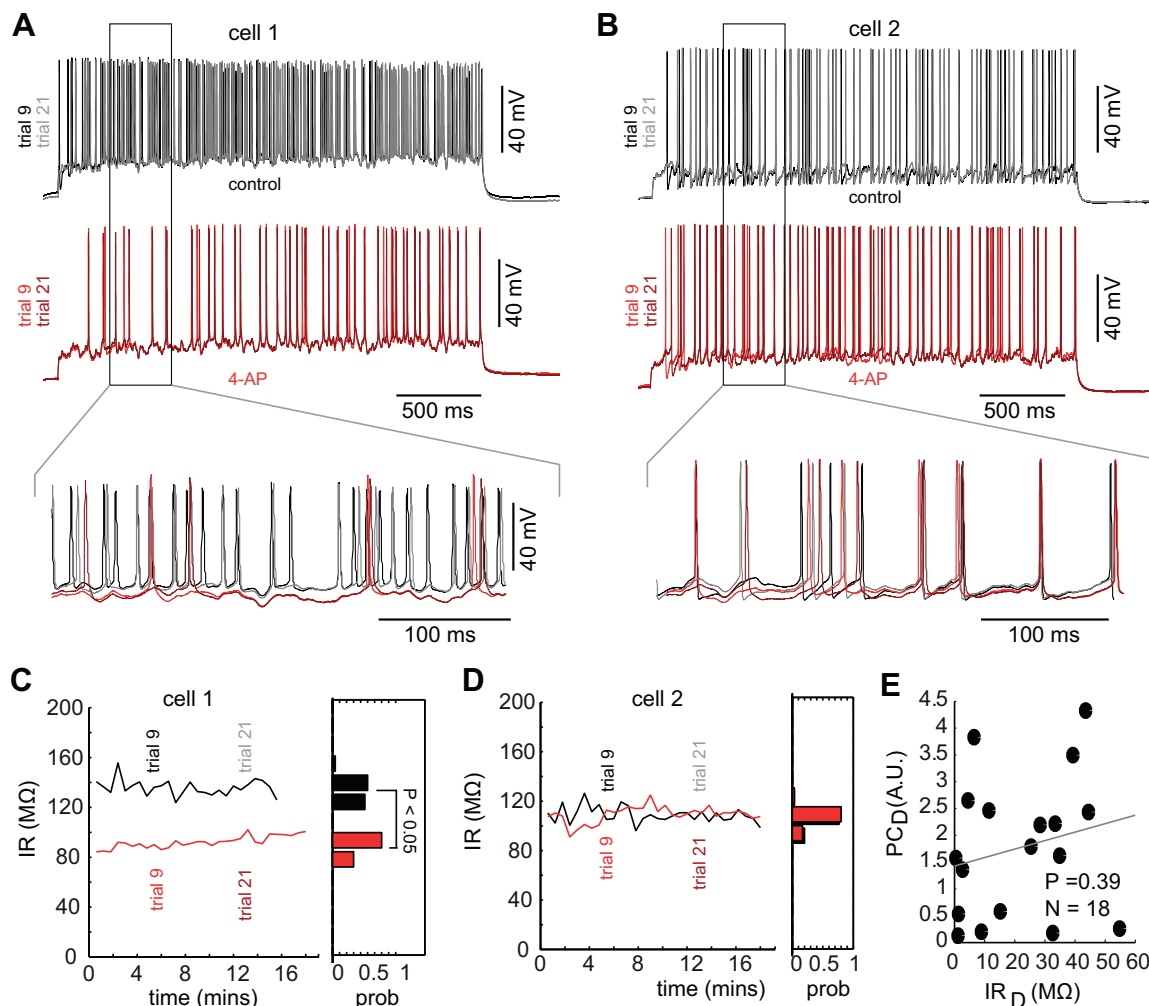


Fig. 6. Changes in spiking following block of 4-AP-sensitive potassium channels are not due solely to changes in input resistance (IR). *A*: spike responses from 2 trials of an example neuron (*trial 9* and *trial 21*) in the control condition (*top*) and following the addition of $5 \mu\text{M}$ 4-AP (*bottom*) where 4-AP affects the neuron's IR. *B*: spike responses from 2 trials of an example neuron (*trial 9* and *trial 21*) in the control condition (*top*) and following the addition of $5 \mu\text{M}$ 4-AP (*bottom*) where 4-AP has no effect on the neuron's IR. *C* and *D*: IR monitored over all trials for the *cell 1* (*C*) and *cell 2* (*D*) and a histogram (right) of the IRs in the control (black) and 4-AP condition (red). *E*: changes in spike train patterns (in the space of PCs) as a function of changes in the IR. AU: arbitrary units.

random and assembled into stimulus locked population responses (Fig. 7*B*). In the example ensemble in the control case, *trial 4* from *cell 1*, *trial 4* from *cell 2*, and *trial 5* from *cell 3* were selected on this example draw. Spikes at each time step (binned into 8-ms windows) were represented as patterns of 1 and 0 s, and the population response, or word, at any given time was represented as vector of 1 and 0 s. In the case of the control response at time S_1 , both *cells 2* and *3* fired, but *cell 1* did not respond, and so the word for that time was [0 1 1] (Fig. 7*B*, *top*). In the same way, words were calculated for the responses of the same three cells in the presence of 4-AP. In this example, the population response was generated by drawing *trial 4* from *cell 1*, *trial 5* from *cell 2*, and *trial 2* from *cell 3*. For the same population, to the same stimulus at time S_1 , the response was [1 0 1], where both *cells 1* and *3* responded, but *cell 2* did not (Fig. 7*B*, *bottom*). This process of generating words at each stimulus time (S_n) was done repeatedly to estimate the distribution of words that occurred for the ensemble. In addition, the distribution of possible words at all times was calculated by examining the frequency of all the words throughout the whole stimulus presentation. The information

these neural ensembles carried about the stimulus was calculated as the difference between the noise entropy (the former quantity; Osborne et al. 2008; Padmanabhan and Urban 2010) and the total entropy (the latter quantity). This calculation was then repeated from the same neuron populations for the same stimulus after adding 4-AP to understand how differences in 4-AP-sensitive current altered the information rate in the population. Following the addition of 4-AP, the information rate of mitral cell populations significantly decreased compared with control populations of the same size (control: 2-cell population 91.3 ± 18.4 bits/s; 15-cell population = 437.5 ± 15.0 bits/s; 4-AP: 2-cell population = 72 ± 18.2 bits/s; 15-cell population = 397.4 ± 19.3 bits/s; Fig. 8*A*, gray line; $P < 0.005$ for each population size tested; $n = 300$ random combinations of mitral cells per ensemble size). However, the information carried by 3- to 15-cell populations in the 4-AP case was still significantly greater ($P < 0.005$, ANOVA) than the information rate of purely homogeneous ensembles made by assigning different trials of the spike trains from a single cell to each of the cells in the population (Osborne et al. 2008; Padmanabhan and Urban 2010). This indicates that blocking 4-AP-sensitive po-

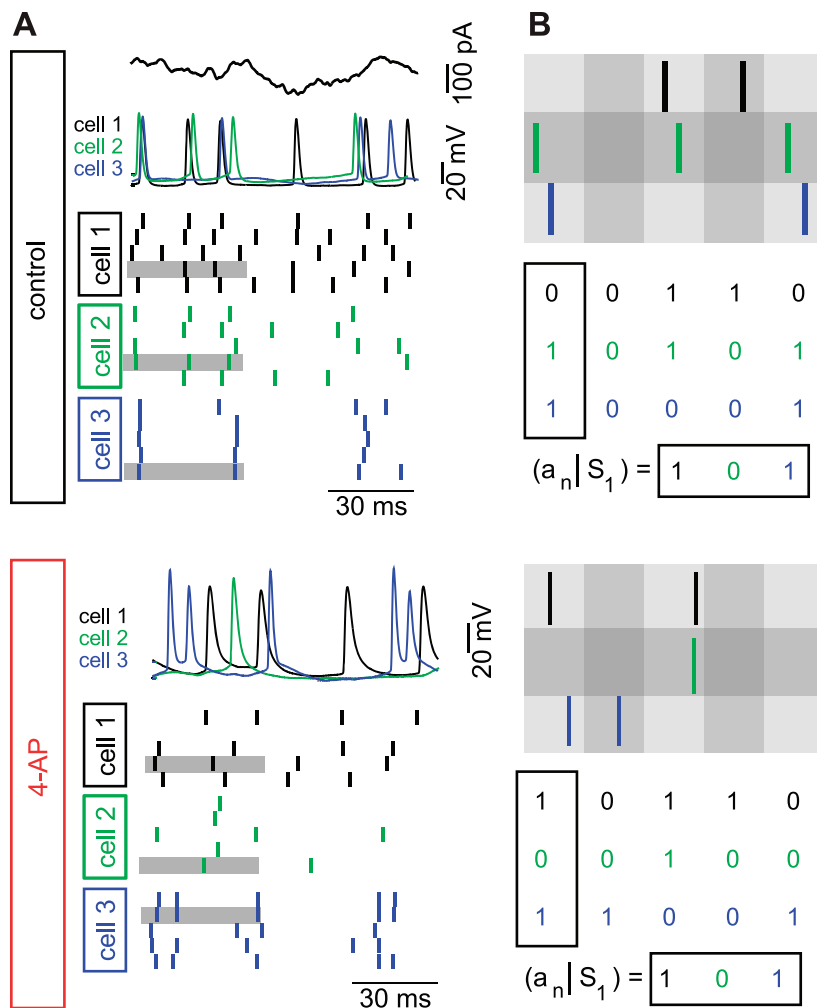


Fig. 7. Information calculation of spike trains from populations of neurons in the control and 4-AP condition. *A*: stimulus (black line at top) and responses from 1 trial of 3 neurons (middle: black, green, and blue) and the rasters for the 5 trials from each of the cells (bottom) in the control condition (black) and following the addition of 4-AP (red). The gray highlighted time segment is enlarged in *B* to show how information is calculated. *B*: Information is calculated by binning the spike trains into 8-ms nonoverlapping bins. Spikes (1 s) and silences (0 s) are assembled across the ensemble of neurons to generate words ([0 1 1]) at each time step for the control population and for the same population following the addition of 4-AP. The process is repeated with different random draws to generate a probability of any given word occurring in response to a stimulus.

tassium channels only partially reduced the useful intrinsic diversity found in the population. The gap between the information in the presence of 4-AP and a purely homogeneous population could be due to the remaining sources of heterogeneity, including the differential expression of other voltage-gated ion channels (Angelo and Margrie 2011).

Encoded information depends on a number of factors in the population spike code, including the diversity in the spike patterns across the population, the reliability of spiking within any given cell, and the firing rates of the neurons in the population. Both noise entropy and total entropy quantify these different features. We therefore plotted, for each ensemble, the information carried in the control condition vs. the information carried by the same population in the 4-AP condition (Fig. 8*B*; $n = 300$ ensembles, for 6-cell populations). The control six-cell ensembles carried 255.5 ± 20.8 bits/s compared with the 4-AP ensembles of the same size that carried 216.6 ± 24.9 bits/s, with only 4% of the 4-AP populations carrying more information than their control counterparts. To determine what caused decreases in stimulus encoding when diversity was reduced, we examined the components in the information rate. In the six-cell populations, the mean total entropy dropped significantly ($P < 0.005$, ANOVA) from 600.9 ± 48.7 to 557.5 ± 48.3 bits/s (Fig. 8*C*, left) with the addition of 4-AP. By contrast, the mean noise entropy, was unchanged by addition of 4-AP (345.4 ± 37.2 bits/s in control vs. 340.9 ± 43.6 bits/s

4-AP; $P = 0.17$, Fig. 8*C*, right). The decreases in information were also not due to differences in firing rates between the two populations, as similar reductions in information were present when firing rate-matched control and 4-AP populations were compared (control = 158.6 ± 11.5 bits/s; 4-AP = 123 ± 7.2 bits/s; $n = 124$ ensembles control; $n = 148$ 4-AP ensembles; $P < 0.005$, ANOVA). Taken together, these data suggest that the change in information rate following the addition of 4-AP was due to a decrease in the diversity of responses the ensemble could generate as evidenced by the reduction in total entropy.

DISCUSSION

In this work, we demonstrate that the cell-to-cell diversity in neurons' spiking can be decreased pharmacologically, thereby changing each cell's spiking properties. The effect of this is to reduce the ability of these populations to carry information about the stimulus. Specifically, we found that among mitral cells in the main olfactory bulb, diversity was conferred in part by a 4-AP-sensitive potassium channel. 4-AP block decreased the response diversity of mitral cells, both from individual animals and across all mice studied. By focusing on mitral cells from different glomeruli, our approach allowed us to investigate how odor information was encoded for by the ensemble integrating features of the stimulus from different glomeruli.

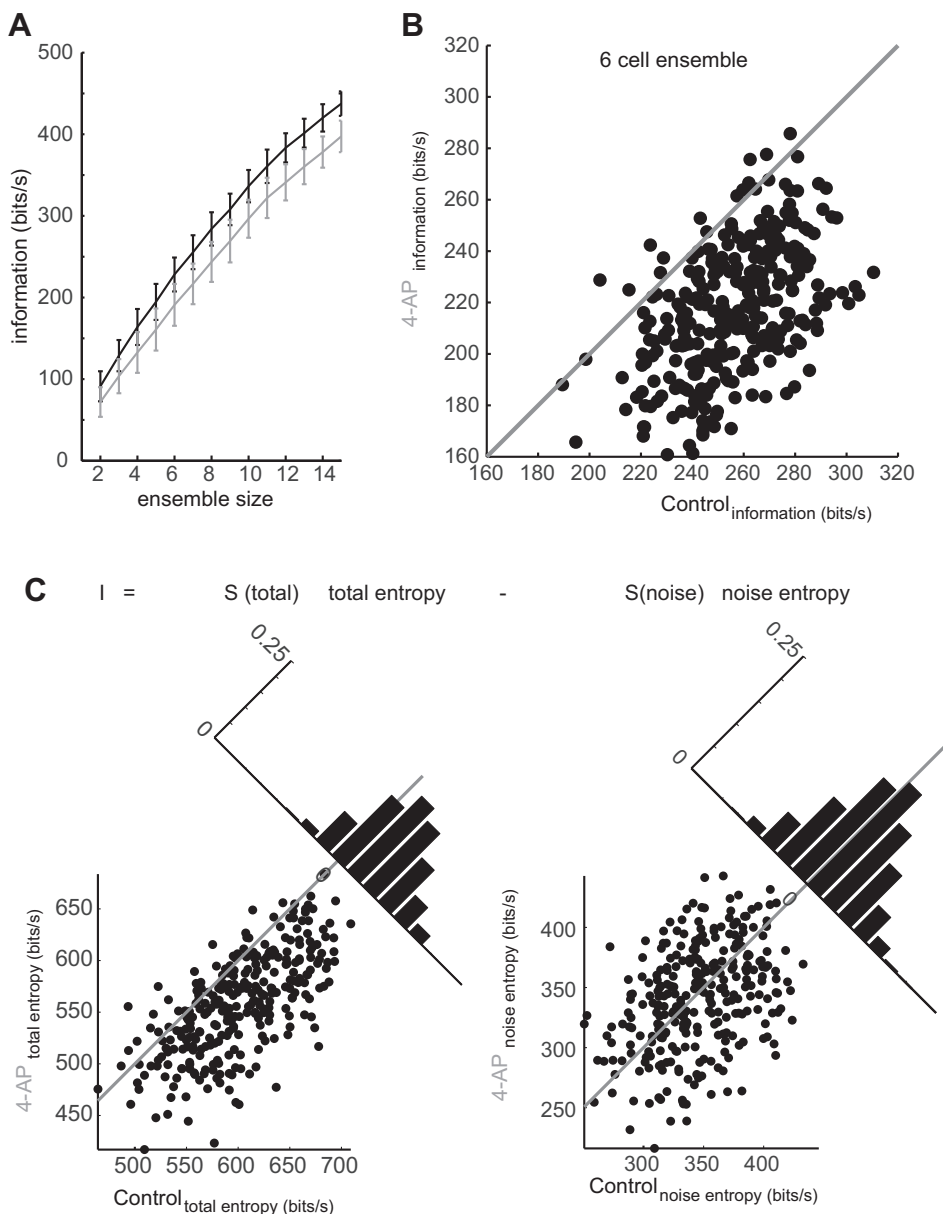


Fig. 8. 4-AP reduces mitral cell information coding in ensembles of neurons. *A*: ensembles of mitral cells made less diverse through block of 4-AP-sensitive potassium channels (gray) carry less information than the same ensembles in the control condition (black) across an array of population sizes (error bars are SD). *B*: information in control populations plotted against the information carried by the same populations in the 4-AP condition and the distribution of this relationship along the orthonormal axis of the unity line. *C*: components of information, the total entropy (*left*) and noise entropy (*right*). For each, the entropy in the control condition is plotted vs. the entropy in the 4-AP condition, for total entropy (*left*) and noise entropy (*right*).

Abolishing this source of diversity pharmacologically resulted in a 21% decrease in information carried by two cell populations and a 10% decrease in information in populations of 15 mitral cells. Although 4-AP, even in the low concentrations we used can have nonspecific effects, previous work has demonstrated that the K_v potassium channel currents constitute the dominant outward currents in the olfactory bulb (Fadool and Levitan 1998). As a result, the 4-AP effect we observed is likely to affect these channels and is consistent with previous work showing that 4-AP-sensitive potassium currents are critical for generating spike clusters and may gate the how mitral cells encode for stimuli in the theta range (Balu et al. 2004). However, 4-AP-sensitive potassium channels are only one component of a mixture of other channels that are differentially expressed by mitral cells, including the hyperpolarization-evoked sag potential and $I(h)$ current that may act on a slower time scale (Angelo et al. 2012). Diversity could therefore further be affected by the combinatorial interactions among

these channels. Different levels of current that passed through both 4-AP-sensitive potassium channels and $I(h)$ channels together may make populations more or less diverse, depending on their respective expression profiles. The impact of biophysical diversity on neuronal function, in the way we measure it in this study by studying the effect of the 4-AP blocker on channel currents, is only one part of a more complex space of diversity that undoubtedly includes differences in the expression of channels at the level of transcription and translation, posttranslational modification, and trafficking of channels in and out of the membrane. For example, differential expression and or channel phosphorylation (Fadool and Levitan 1998) may each contribute to the diversity observed at the level of the potassium current in mitral cells as has been reported. By remaining agnostic about these other sources of diversity, and instead selecting one component of the cell's physiological output, its response to complex inputs currents, we could target currents through channels selective to 4-AP

and then study how this affects the ways stimulus information is encoded. We note the decreases in information following 4-AP we observe do not drop to that of purely homogeneous populations (Padmanabhan and Urban 2010), suggesting that sources of diversity described above may also contribute to the heterogeneity of neurons and, therefore, their response variability.

The diversity across a population of all recorded mitral cells (from different glomeruli, in different animals) is likely to be reflective of the diversity within individual animals based on our results but may also be different from the diversity found in networks of sister mitral cells that receive input in the same glomerulus, as recent work implies (Angelo et al. 2012). However, given that mitral cells associated with many glomeruli participate in the representation of a given odor stimulus, heterogeneities of both sister and nonsister mitral cells are likely to be important in odor coding to downstream targets (Miyamichi et al. 2011). Notably, cells in the piriform cortex are one of the targets of mitral cell axons from different glomeruli. Our work describes how information may be relayed to these piriform neurons as a result of the diversity across the population of mitral cells from different glomeruli. As a result, our method of information calculation generalizes to these cases, showing that even if different glomeruli have different amounts of diversity, the information rates of the ensembles should correlate to the diversity of the mitral cells belonging to those ensembles.

Finally, we considered the case wherein neurons are receiving perfectly correlated inputs. The optimal diversity for encoding stimuli may be different when input correlations are lower or the neurons fire unreliably. Nonetheless, our work points not simply to the relationship between diversity and coding, but also provides a framework to explore how different amounts of diversity among neurons affect the way stimuli are encoded.

The role of channel diversity is also likely not restricted to information coding. Intrinsic heterogeneity has recently been shown to limit correlation-induced neuronal synchrony (Burton et al. 2012). Synchronous neuronal oscillations are found throughout the brain, and mechanisms thought to give rise to these oscillations include coupled or correlated input (Salinas and Sejnowski 2002). As biophysical diversity limits the degree of synchronization (Burton et al. 2012), heterogeneity may also play a role in shaping network dynamics in circuits.

In our work, we address coding broadly by representing the different effects of channel diversity on spiking activity in a single value, the population's information rate. This general result highlights the net effect of diversity on potential neuronal codes. Different systems may tailor the degree of diversity across the neural population to specific coding tasks. Notably, biophysical diversity has been identified in a number of other systems across many different species including in the communication signals of the electric fish (Marsat et al. 2012), the auditory brainstem of the chick (Kuba et al. 2005), the spinal ganglion neurons of the cochlea (Adamson et al. 2002), and the grid cells in the entorhinal cortex in mammals (Giocomo et al. 2009). In some of these instances such as in the electric fish, diversity of intrinsic properties allows the system to route behaviorally relevant information differently, using different populations of lateral line lobe pyramidal neurons to represent courtship vs. aggressive behaviors separately (Marsat and

Maler 2010). In other instances, such as the chick brain stem, the differential expression of $K_v1.2$ potassium channels in the nucleus laminaris may allow some cells to serve as coincidence detectors, thereby affording the animal higher resolution sound localization. Additionally, the differential expression of HCN neurons as a gradient in the entorhinal cortex may set the organization of the receptive fields of the grid cells (Giocomo et al. 2011). Each of these examples illustrates how diversity across populations of neurons may facilitate how sensory information is represented and processed in the nervous system. As a result, intrinsic biophysical diversity could reflect a general theme, across not only different sensory systems, but also different species, for optimal stimulus encoding.

In the case of the olfactory bulb, the coverage of a large coding space of odors may require intrinsic diversity in the mitral cell population. Alternatively, if stimuli are noisy, or stimuli need to be encoded with highly correlated firing for efficient downstream information transmission, diversity may be reduced. In this respect, intrinsic biophysical heterogeneity may be as important to neuronal coding as the connectivity of neurons (Assisi et al. 2011) or their dendritic morphology (Mainen and Sejnowski 1996; Jia et al. 2011). Diversity could either be increased or decreased depending on the coding strategy employed by the network and may, therefore, be another feature of the neuronal circuit that can be manipulated by the nervous system to encode stimuli.

ACKNOWLEDGMENTS

We thank Shreejoy Tripathy, Richard Gerkin, Cian O'Donnell, and members of the Urban Laboratory for helpful comments on this manuscript.

Current address of K. Padmanabhan: Crick Jacobs Center for Theoretical and Computational Biology, Salk Institute, La Jolla, CA 92037.

GRANTS

This work was supported by National Institute of Deafness and Other Communications Disorders Grants DC-R01-005798 and DC-R01-011184 (to N. N. Urban). K. Padmanabhan is supported by National Institute of Mental Health Grant K99-MH 101634 and a Crick-Jacobs Junior Fellowship.

DISCLOSURES

No conflicts of interest, financial or otherwise, are declared by the author(s).

AUTHOR CONTRIBUTIONS

Author contributions: K.P. and N.N.U. conception and design of research; K.P. performed experiments; K.P. analyzed data; K.P. interpreted results of experiments; K.P. prepared figures; K.P. drafted manuscript; K.P. and N.N.U. edited and revised manuscript; K.P. and N.N.U. approved final version of manuscript.

REFERENCES

- Adamson CL, Reid MA, Davis RL. Opposite actions of brain-derived neurotrophic factor and neurotrophin-3 on firing features and ion channel composition of murine spiral ganglion neurons. *J Neurosci* 22: 1385–1396, 2002.
- Angelo K, Margrie TW. Population diversity and function of hyperpolarization-activated current in olfactory bulb mitral cells. *Sci Rep* 1: 50, 2011.
- Angelo K, Rancz EA, Pimentel D, Hundahl C, Hannibal J, Fleischmann A, Pichler B, Margrie TW. A biophysical signature of network affiliation and sensory processing in mitral cells. *Nature* 488: 375–378, 2012.
- Assisi C, Stopfer M, Bazhenov M. Using the structure of inhibitory networks to unravel mechanisms of spatiotemporal patterning. *Neuron* 69: 373–386, 2011.

- Balu R, Larimer P, Strowbridge BW.** Phasic stimuli evoke precisely timed spikes in intermittently discharging mitral cells. *J Neurophysiol* 92: 743–753, 2004.
- Bryant HL, Segundo JP.** Spike initiation by transmembrane current: a white-noise analysis. *J Physiol* 260: 279–314, 1976.
- Burton SD, Ermentrout GB, Urban NN.** Intrinsic heterogeneity in oscillatory dynamics limits correlation-induced neural synchronization. *J Neurophysiol* 108: 2115–2133, 2012.
- Cang J, Issacson, JS.** In vivo whole-cell recording of odor-evoked synaptic transmission in the rat olfactory bulb. *J Neurosci* 23: 4108–4116, 2003.
- Carey RM, Wachowiak M.** Effect of sniffing on the temporal structure of mitral/tufted cell output from the olfactory bulb. *J Neurosci* 31: 10615–10626, 2011.
- Chelaru MI, Dragoi V.** Efficient coding in heterogeneous neuronal populations. *Proc Natl Acad Sci USA* 105: 16344–16349, 2008.
- Connor JA, Stevens CF.** Prediction of repetitive firing behaviour from voltage clamp data on an isolated neurone soma. *J Physiol* 13: 31–53, 1971.
- Dhawale AK, Hagiwara A, Bhalla US, Murthy VN, Albeanu DF.** Non-redundant odor coding by sister mitral cells revealed by light addressable glomeruli in the mouse. *Nat Neurosci* 13: 1404–1412, 2010.
- Fadool DA, Levitan IB.** Modulation of olfactory bulb neuron potassium current by tyrosine phosphorylation. *J Neurosci* 18: 6126–6137, 1998.
- Galán RF, Ermentrout GB, Urban NN.** Optimal time scale for spike-time reliability: theory, simulations, and experiments. *J Neurophysiol* 99: 277–283, 2008.
- Giocomo LM, Hasselmo ME.** Knock-out of HCN1 subunit flattens dorsal-ventral frequency gradient of medial entorhinal neurons in adult mice. *J Neurosci* 29: 7625–7630, 2009.
- Giocomo LM, Hussaini SA, Zheng F, Kandell ER, Moser MB, Moser EI.** Grid cells use HCN1 channels for spatial scaling. *Cell* 147: 1159–1170, 2011.
- Ghosh S, Larson SD, Hefzi H, Marnoy Z, Cutforth T, Dokka K, Baldwin KK.** Sensory maps in the olfactory cortex defined by long-range viral tracing of single neurons. *Nature* 472: 217–220, 2011.
- Häusser M, Mel B.** Dendrites: bug or feature? *Curr Opin Neurobiol* 13: 372–383, 2003.
- Jia H, Rochefort NL, Chen X, Konnerth A.** Dendritic organization of sensory input to cortical neurons in vivo. *Nature* 464: 1307–1312, 2010.
- Kuba H, Yamada R, Fukui I, Ohmori H.** Tonotopic specialization of auditory coincidence detection in nucleus laminaris of the chick. *J Neurosci* 25: 1924–1934, 2005.
- Mainen ZF, Sejnowski TJ.** Influence of dendritic structure on firing pattern in model neocortical neurons. *Nature* 382: 363–366, 1996.
- Marsat G, Maler L.** Neural heterogeneity and efficient population codes for communication signals. *J Neurophysiol* 104: 2543–2555, 2010.
- Marsat G, Longtin A, Maler L.** Cellular and circuit properties supporting different sensory coding strategies in electric fish and other systems. *Curr Opin Neurobiol* 22: 686–692, 2012.
- Meister M, Bonhoeffer T.** Tuning and topography in an odor map of the rat olfactory bulb. *J Neurosci* 21: 1351–1360, 2001.
- Miyamichi K, Amat F, Moussavi F, Wang C, Wickersham I, Wall NR, Taniguchi H, Tasic B, Huang ZJ, He Z, Callaway EM, Horowitz MA, Luo L.** Cortical representations of olfactory input by trans-synaptic tracing. *Nature* 472: 191–196, 2011.
- Osborne LC, Palmer SE, Lisberger SG, Bialek W.** The neural basis for combinatorial coding in a cortical population response. *J Neurosci* 28: 13522–13531, 2008.
- Padmanabhan K, Urban NN.** Intrinsic biophysical diversity decorrelates neuronal firing while increasing information content. *Nat Neurosci* 13: 1276–1282, 2010.
- Rubin BD, Katz LC.** Optical imaging of odorant representations in the mammalian olfactory bulb. *Neuron* 23: 499–511, 1999.
- de Ruyter van Steveninck RR, Lewen GD, Strong SP, Koberle R, Bialek W.** Reproducibility and variability in neural spike trains. *Science* 275: 1805–1808, 1997.
- Salinas E, Sejnowski TJ.** Integrate-and-fire neurons driven by correlated stochastic input. *Neural Comput* 14: 2111–2155, 2002.
- Shamir M, Sompolinsky H.** Implications of neuronal diversity on population coding. *Neural Comput* 18: 1951–1986, 2006.
- Smear M, Shusterman R, O'Connor R, Bozza T, Rinberg D.** Perception of sniff phase in mouse olfaction. *Nature* 479: 397–400, 2011.
- Sosulski DL, Bloom ML, Cutforth T, Axel R, Datta SR.** Distinct representations of olfactory information in different cortical centres. *Nature* 472: 213–216, 2011.
- Stocks N.** Suprathreshold stochastic resonance in multilevel threshold systems. *Phys Rev Lett* 84: 2310–2313, 2000.
- Strong SP, de Ruyter van Steveninck RR, Bialek W, Koberle R.** On the application of information theory to neural spike trains. *Pac Symp Biocomput* 621: 32, 1998.
- Tripathy SJ, Padmanabhan K, Gerkin RC, Urban NN.** Intermediate intrinsic diversity enhances neural population coding. *Proc Natl Acad Sci USA* 110: 8248–8253, 2013.
- Urban NN, Sakmann B.** Reciprocal intraglomerular excitation and intra- and interglomerular lateral inhibition between mouse olfactory bulb mitral cells. *J Physiol* 542: 355–367, 2002.